Changes in spectral fluorescence properties of a near-infrared photosensitizer in a nanoform as a coating of an optical fiber neuroport

Yulia Maklygina, Igor Romanishkin, Aleksey Skobeltsin, Dina Farrakhova, Kharnas Sergej, Lina Bezdetnaya, Victor Loschenov

photonics

MDPI

Article

Changes in Spectral Fluorescence Properties of a Near-Infrared Photosensitizer in a Nanoform as a Coating of an Optical Fiber Neuroport

Yuliya Maklygina [1,*], Igor Romanishkin [1], Aleksej Skobeltsin [1], Dina Farrakhova [1], Sergej Kharnas [2], Lina Bezdetnaya [3,4] and Victor Loschenov [1,5]

1 Prokhorov General Physics Institute of the Russian Academy of Sciences, 119991 Moscow, Russia; igor.romanishkin@nsc.gpi.ru (I.R.); skoaleksej@yandex.ru (A.S.); farrakhova.dina@mail.ru (D.F.); loschenov@mail.ru (V.L.)
2 N.N. Burdenko Clinic of the Faculty of Surgery, N.N. Burdenko Clinic (Director-Acad. of RAMS A.F. Chernousov) I.M. Sechenov Medical Academy, 119121 Moscow, Russia; kharnas_s_s@staff.sechenov.ru
3 Centre de Recherche en Automatique de Nancy, CNRS, Université de Lorraine, 54519 Vandoeuvre-lès-Nancy, France; l.bolotine@nancy.unicancer.fr
4 Institut de Cancérologie de Lorraine, 54519 Vandoeuvre-lès-Nancy, France
5 Institute of Engineering Physics for Biomedicine, National Research Nuclear University MEPhI, 115409 Moscow, Russia
* Correspondence: mclygina@nsc.gpi.ru; Tel.: +7-977-803-76-27

Abstract: In this work, we tested a new approach to assess the presence of inflammatory process in the implant area using spectral methods and the technique of fiber fluorescence analysis of photosensitizers in nanoform. First of all, the spectral characteristics of the photosensitizer when interacting with the porous surface of the implant, based on hydroxyapatite under in vitro and in vivo conditions, were determined. Thus, it was shown that spectral characteristics of photosensitizers can be used for judgement on the process of inflammation in the implant area and thus on the local presence of the immunocompetent cells. The analysis was performed at a sufficient depth in the biotissue by using the near-infrared spectral region, as well as two different methods: fiber-based laser spectroscopy and fiber-optic neuroscopy, which served to monitor the process and regular fluorescence diagnosis of the studied area. Fluorescence spectroscopic analysis was performed on experimental animals in vivo, i.e., under conditions of active immune system intervention, as well as on cell cultures in vitro in order to judge the role of the immune system in the interaction with the implant in comparison. Thus, the aim of the study was to determine the relationship between the fluorescence signal of nanophotosensitizers in the near infrared spectral region and its parameters with the level of inflammation and the type of surface with which the photosensitizer interacts in the implant area. Thus, fiber-optic control opens up new approaches for further diagnosis and therapy in the implant area, making immune cells a prime target for advanced therapies.

Keywords: fiber-optic neurosystem; laser spectroscopy; laser confocal microscopy; nanophotosensitizers; infrared region; hydroxyappatite; macrophages; glioma

Citation: Maklygina, Y.; Romanishkin, I.; Skobeltsin, A.; Farrakhova, D.; Kharnas, S.; Bezdetnaya, L.; Loschenov, V. Changes in Spectral Fluorescence Properties of a Near-Infrared Photosensitizer in a Nanoform as a Coating of an Optical Fiber Neuroport. *Photonics* **2021**, *8*, 556. https://doi.org/10.3390/photonics8120556

Received: 1 November 2021
Accepted: 3 December 2021
Published: 6 December 2021

1. Introduction

Optical methods also have many advantages in the treatment of various brain pathologies due to the possibility of selective exposure to altered tissues containing a contrasting substance sensitive to radiation at certain wavelengths, leading to photochemical, photothermal and photobiological reactions in the tissues [1]. The ability of cells of different morphologies to accumulate photosensitizers (PS) in different ways opens up the possibility of their optical non-invasive differentiation and deactivation under the influence of radiation into the absorption band of the photosensitizer of endogenous and exogenous nature. It is immune cells that can accumulate photosensitizers several times more than

tumor cells—up to 9 times [2], which is associated with differences in the set of effector molecules, metabolism and phagocytosis [3–5].

Moreover, the use of nanocomposites that fluoresce in the far-red and near infrared (IR) spectral range and have a phototoxic effect opens up new opportunities for the diagnosis and therapy of deep-seated tumors [6–8].

Despite the fact that the developed neuro-optical system provides constant access to the brain [9], namely, to the tumor bed, the effect of laser radiation (FD and PDT) can spread to tissues that are within a maximum radius of 1–2 cm, provided the PS of far-red and near-infrared spectral ranges are used. Along with directional studies of photosensitizers with intense absorption band in the far red and near-infrared spectral regions, new molecular nanocrystals based on organic molecules derived from already known photosensitizers were investigated.

The interest lies in the fact that crystalline nanoparticles do not fluoresce but can be used as an "indicator" of a pathological process, as under the influence of external factors they start to exhibit the properties of free aluminum phthalocyanine and bacteriochlorine molecules, respectively [10,11]. A possible mechanism of fluorescence occurrence lies in the pathological biotissues, whose microflora and immune system response differ from those of healthy biotissues. The most probable mechanism of fluorescence occurrence is the transition of nanoparticle surface molecules from para-position to ortho-position due to macrophage enzymes, which cause the appearance of fluorescent and photoactive properties of the nanoparticle [1]. The decrease in the fluorescence intensity of nanoparticles after exposure to light may be due to the breakdown of the bonds between the surface molecules and macrophage enzymes that transferred the surface molecules to the ortho-position, whereupon the surface molecules pass into the para-position again and the fluorescent and photoactive properties of nanoparticles disappear.

The promising use of the investigated PS nanoparticles is due to a number of their advantages:

(1) The nanoparticle has absorption and fluorescence peaks in the far-red region of the spectrum, which allows an increase in the depth of photodynamic action on pathological tissues;
(2) It can show itself as an "indicator" of a pathological process, having the ability to photoactivate under conditions of interaction with pathological agents;
(3) The tropicity of the drug to tumor tissues can be increased by using nanoscale particles with diameters of 100–220 nm.

In this work, nanoparticles of aluminum phthalocyanine and bacteriochlorine were used to study their spectral-optical properties in contact with an implant based on hydroxyapatite (a material replicating bone tissue) [12–18] and the cells of bio tissue.

2. Materials and Methods

The monitoring of cell growth processes consists in the detection by fluorescence spectroscopy of areas with increased fluorescence intensity caused either by an increased concentration of accumulating photosensitizer molecules in the case of glioma or by a high concentration of nerve cells labelled with special fluorescent proteins. The study was performed on experimental animals (sexually mature female Wistar rats weighing 200–220 g) with an induced brain tumor. Animal care protocols were used in accordance with the guidelines of the European Convention for the Protection of Vertebrate Animals used for Experimental and Other Scientific Purposes (Strasbourg, 18.III.1986).

In order to provide access to the tumor bed, an intracranial neurosystem with an internal fiber-optic structure was preliminarily implanted. The fiber-optic neurosystem thereby made it possible to perform in vivo measurements [9].

In vivo and in vitro PS accumulation studies were carried out with a laser spectroanalyzer using PS: aluminum phthalocyanine and meso-tetra (3-pyridyl) bacteriochlorine (hereafter bacteriochlorine) in nano-form. In this work, the objects of interest were far-red and near-IR PS in nano-form: aluminum phthalocyanine (AlPc) and bacteriochlorine (Bch).

The methodology for the preparation of colloidal solutions was identical with the only difference as which starting substance was used. The initial material for the preparation of nanoparticles, polycrystalline powder AlPc and Bch, was obtained from FSUE "NIOPIK". An aqueous colloidal solution of AlPc and Bch molecular nanocrystals was prepared during the study. In preparation for the experiment, polycrystalline powder was added to distilled water until a concentration of 1 mg/mL was obtained. The resulting suspension was dispersed in a Bandelin SONOPLUS HD2070 ultrasonic homogenizer. Using a multi-angle spectrometer of dynamic light scattering photocor complex (Russia), the average particle diameter in the aqueous colloid was 220–240 nm. The spectrometer of dynamic light-scattering measures the hydrodynamic radius, which significantly depends on several parameters: the zeta potential of the nanoparticle, its shape, temperature and viscosity of the environment. Therefore, the values obtained are used as a guide.

To determine the fluorescence spectra in vivo, an experimental setup based on the following modules was assembled: LESA-01-BIOSPEK fiber-optic spectroanalyzer; computer with software; laser with filters and optical fiber input system as a light source to excite fluorescence (The radiation source is selected according to the absorption spectrum of the substance). Y-shaped fiber-optic diagnostic probe including receiving and irradiating fibers. Radiation from the laser source enters the input end of the diagnostic fiber and is applied to the sample under examination. The optical path of photons in the biotissue has a banana-shaped trajectory to the receiving fiber connected to the spectrometer, after which, the signal from the spectrometer is received by the PC and processed by the UnoMomento software. The structure of the optical fiber used to deliver radiation from the light source to the sample as well as from the sample to the spectrum analyzer minimizes radiation loss due to scattering. Spectroanalyzer LESA-01-BIOSPEC, having spectral range of 400–1100 nm, is accompanied by software that enables calculation of the fluorescence spectrum of investigated samples with normalization on hardware function, received on the basis of spectrum of calibrated light source.

Studies of PS accumulation under in vitro conditions were carried out on cell cultures using a laser scanning confocal microscope. Fluorescence kinetic characteristics were studied using a laser scanning microscope LSM-710-NLO (Carl Zeiss, Jena, Germany). Excitation was performed with a femtosecond pulsed laser Chameleon Ultra II (80 MHz, pulse duration 140 fs, wavelength range 690–1060 nm, Coherent Inc., Santa Clara, CA, USA), wavelength 980 nm. Images were acquired with the following scanning modes: 20× objective, scan area size 400 × 400 μm, resolution 1024 × 1024 pixels, scan speed 1.27–3.15 μs/pixel. Total image acquisition time is 18.7 s. The average power density measured with a coherent power meter (USA) at the sample location level was 5.42 mW, with a power density of 7 kW/cm^2 per scanning spot, 10 μm in size.

3. Results

3.1. Studies of the Spectral Fluorescence Properties of Photosensitizers in Nanoform on the Surface of Hydroxyapatite

To study the dynamics of photosensitizer accumulation in the porous structure of the hydroxyapatite that makes up the implant, a series of experimental researches were performed [9]. The process of implant biointegration was simulated under in vitro conditions as follows (Figure 1):

Stage 1: spectral-luminescent properties of nanoparticles in interaction with the surface molecules of hydroxyapatite were studied taking into account the fact that free nanocrystals in aqueous colloid have no ability to luminescence;

Stage 2: spectral luminescence properties of nanoparticles under conditions of interaction of implant surface (hydroxyapatite with surface layer of PS nanoparticles) with polar solvent dimethyl sulfoxide (DMSO) were studied, which simulated the interaction process with biocomponents (immunocompetent cells, bacteria, etc., under in vivo conditions);

Stage 3: spectral and luminescent properties were studied after washout of polar solvent from the surface of the implant porous structure by water dispersion in an ultrasonic homogenizer in order to exclude the possibility of its washout over time.

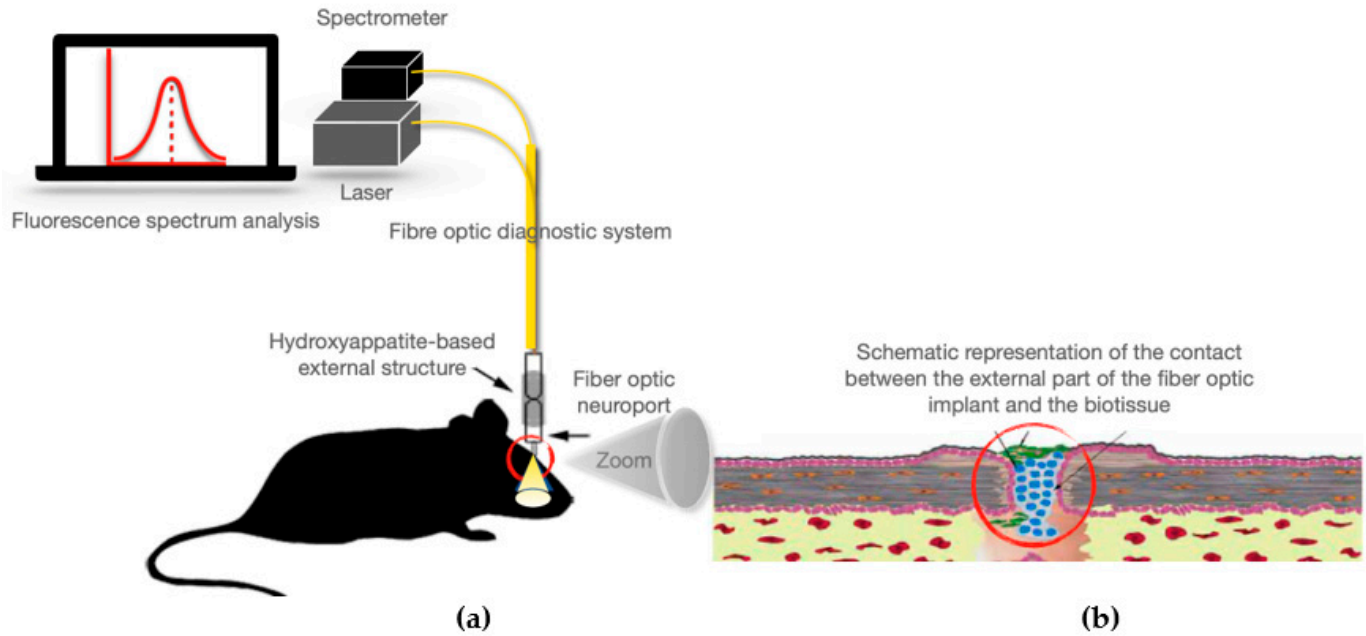

Figure 1. (**a**) Schematic representation of an experimental model for investigating intratissue processes after implantation. (**b**) Schematic representation of the contact between the external part of the hydroxyappatite-based implant and the biotissue at the implant site.

The results of the stepwise exposure of the implant surface are shown in the form of luminescence spectra in Figures 2 and 3 for the nBch and nPcAl surface-coated samples, respectively.

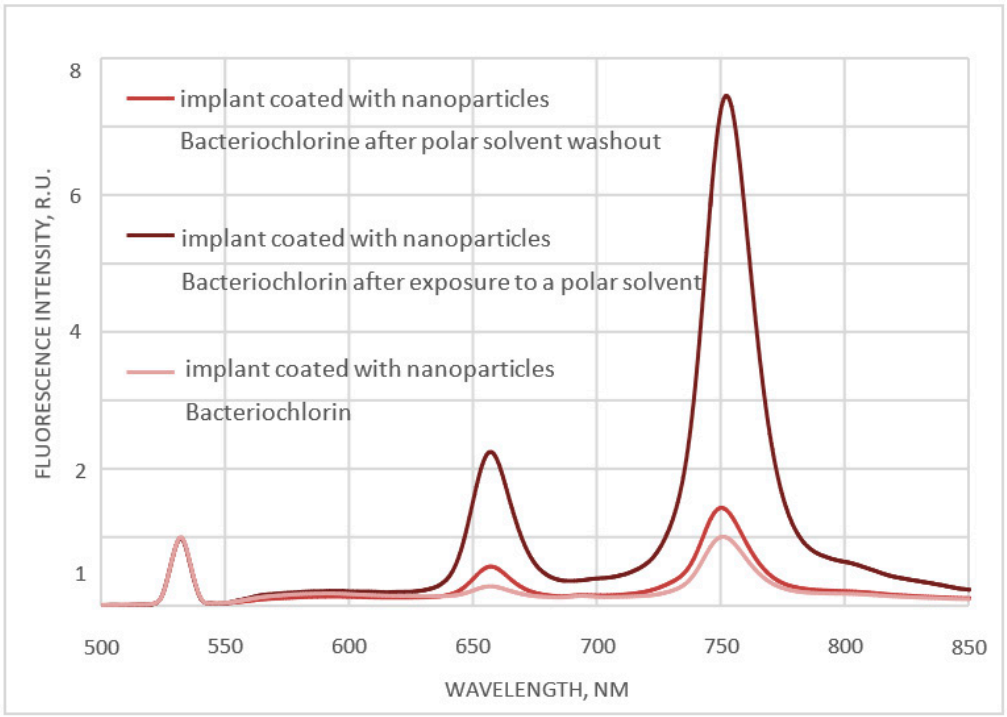

Figure 2. Luminescence spectrum of a hydroxyapatite-based implant coated with bacteriochlorine nanoparticles under different conditions (λex = 532 nm).

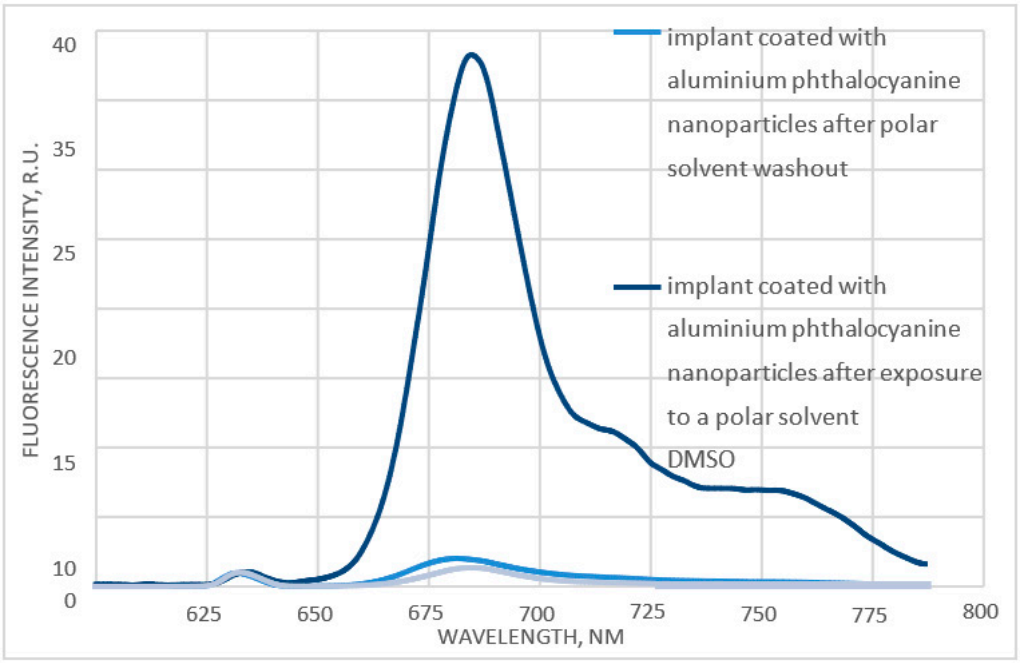

Figure 3. Luminescence spectrum of a hydroxyapatite-based implant coated with aluminum phthalocyanine nanoparticles under different conditions (λex = 632.8 nm).

Analysis of luminescence spectra and luminescence peak dynamics under different conditions for both types of crystalline nanoparticles (bacteriochlorine and aluminum phthalocyanine) shows that PS nanocrystals, initially having no photoactivity, when interacting with surface hydroxyapatite molecules change their spectroscopic properties and acquire the ability to fluoresce. So, crystalline nanoparticles do not fluoresce, but can be used as an "indicator" of the location of surface molecules of nanoparticles, because under the influence of external factors, such as a solvent, for example, they begin to show the properties of free molecules and begin to fluoresce. This phenomenon can probably be explained by the interaction of surface molecules of nanoparticles with the complex and heterogeneous surface structure of hydroxyapatite. Depending on the localization in the porous structure of hydroxyapatite and the nearest environment of the PS nanocrystals, their surface molecules can "lie down", accepting the para-position relative to the nanoparticle surface, or "stand up", accepting the ortho-position, being held on the surface and displaying the spectroscopic properties of the PS solution, which were demonstrated under the interaction conditions of the implant surface with DMSO [19,20]. Washing was carried out for 3 min as statistically it was found that this time is sufficient as the polar solvent reacts quickly with the photosensitizer molecules. Dimethyl sulfoxide (DMSO) is the most commonly used nonaqueous solvent and is classified as class 3 (nontoxic). As the photosensitizers tested are water soluble, DMSO was used to dissolve them. In solution, solvent molecules surrounding the fluorophore in the ground state have dipole moments that can interact with the dipole moment of the fluorophore, creating an ordered distribution of solvent molecules around the fluorophore [21]. Quantitative studies of fluorescence in a complex system of porous structure revealed fluctuating intensities, which presumably resulted from the most probable mechanism of fluorescence increase in this case is the transition of surface molecules of photosensitizer nanoparticles from para-position to ortho-position due to the influence of solvent molecules, which results in the increase of fluorescent and photoactive properties of nanoparticles. In this case, this can presumably be explained by the fact that the para-position is the flat structure of the surface molecules and is more rigid which can increase the stability of the photon-electron excitation transition and reduce the probability of fluorescence excitation. Whereas the ortho-position of molecules in a solvent environment, in a biological environment can affect their instability

and thereby dodge the intensity of fluorescence. The absorption region at wavelengths is explained by the type of dyes under study which correspond to the red and near-infrared region of the spectrum. The dyes under study can absorb photon energy of visible light of a certain wavelength. As they move towards higher energy, they reflexively stop absorbing visible light wavelengths and the transient photoelectrons transfer their energy through the thermal motion of the molecules, passing back to the ground state, whereby the absorption of 400–605 nm wavelength reflexes 605–700 nm red light is observed [22].

Thus, the process of activation of crystalline PS nanoparticles is confirmed by the sharp increase of photoluminescence signal intensity (Figures 2 and 3) at interaction with polar solvent, which allowed imitating the interaction of the implant with the surface layer of PS nanoparticles with biocomponents in vivo.

The study also revealed that the surface molecules of PS nanoparticles have a rather strong interaction with the surface structure of hydroxyapatite, as even by means of aqueous dispersion, it was not possible to achieve washout of nanocrystals from the porous implant structure, which confirms the presence of luminescence signal for both types of nanoparticles after the third stage of exposure (Figures 2 and 3).

In the course of the work, the time dynamics of luminescence spectra of the implant surface based on hydroxyapatite coated with PS nanoparticles was also studied. The analysis of time-resolved luminescence spectra for both types of crystalline nanoparticles (nBch and nPcAl) showed that initially photoinactive PS nanocrystals acquire luminescence ability when interacting with the surface hydroxyapatite molecules. However, the intensity of the luminescence peak is changed in time under the influence of the exciting laser radiation of the appropriate wavelength (nBch: λex = 532 nm, nPcAl: λex = 632.8 nm).

The luminescence spectrum of the hydroxyapatite-based implant surface coated with nBch, when excited by laser radiation (λex = 532 nm) has two luminescence peaks: λem = 758 nm and λem = 654 nm. When continuously exposed to the excitation laser radiation, the intensity of the luminescence peaks varies with time, with the luminescence signal intensity of the peak corresponding to λem = 654 nm increasing with time, while the luminescence signal intensity of the peak corresponding to λem = 758 nm decreases with time (Figure 4).

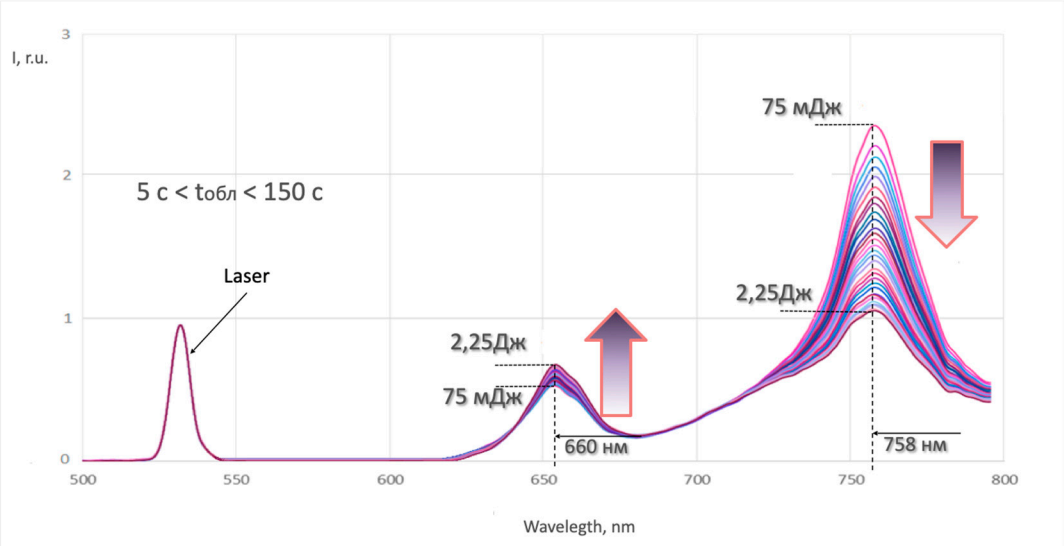

Figure 4. Time course of the luminescence spectrum of a hydroxyapatite-based implant coated with bacteriochlorine nanoparticles (λex = 532 nm).

Apparently, depending on the duration of exposure, which corresponds to a change in the energy level of the reported system, the surface molecules change their position relative to each other and the surface structure of hydroxyapatite, exhibiting the spectroscopic properties of bacteriochlorine (λem = 758 nm) or chlorine (λem = 654 nm) solution.

It should be noted that this process is reversible, indicating the impossibility of structural change in the photosensitizer molecule itself, namely, the formation of an independent chlorine molecule. Figure 5 shows that the difference in structure between bacteriochlorine and chlorine molecules lies in the presence of another double bond in the chlorine structural formula. Therefore, it is likely that, under the influence of excitation laser radiation, two nearby bacteriochlorine molecules may interact by forming a common temporary double bond between them, which breaks down in the absence of excitation laser radiation. So, this double bond, which distinguishes the chlorine molecule from the bacteriochlorine molecule, could thus be induced, as the surface molecules of the nanoparticles change their position relative to the hydroxyapatite surface due to laser energy, in particular thermal diffusion. Due to its porosity, this becomes quite a complex interaction, as the pore is a surface which can surround the nanoparticles from all sides. In this case, one of the molecules may exhibit the spectroscopic properties of a chlorine molecule. Based on these results, it was concluded that bacteriochlorine nanoparticles interact both in pairs with each other and with the complex porous structure of hydroxyapatite. Depending on the nature and strength of the interaction, as well as the localization and environment of the nanoparticles, they can take a different position in relation to each other and the surface structure of hydroxyapatite, while changing the spectroscopic properties, but without undergoing irreversible changes in the structure of the molecule.

Figure 6 shows the dynamics of the luminescence spectrum of the implant surface based on hydroxyapatite, coated with nPcAl. The luminescence spectrum of the implant surface on the hydroxy-apatite base, coated with nPcAl, at the excitation by laser radiation λex = 632.8 nm has the luminescence peak λem = 682 nm. When constant continuous exposure to excitation laser radiation for some period of time the intensity of the luminescence peak decreases in time.

Apparently, as in the case of nBch, during irradiation the surface molecules change their position relative to each other and to the surface structure of hydroxyapatite, resulting in spectral changes. It should be noted that this process is reversible, which indicates that there is no structural change in the nanophotosensitizer molecule itself or dye burnout.

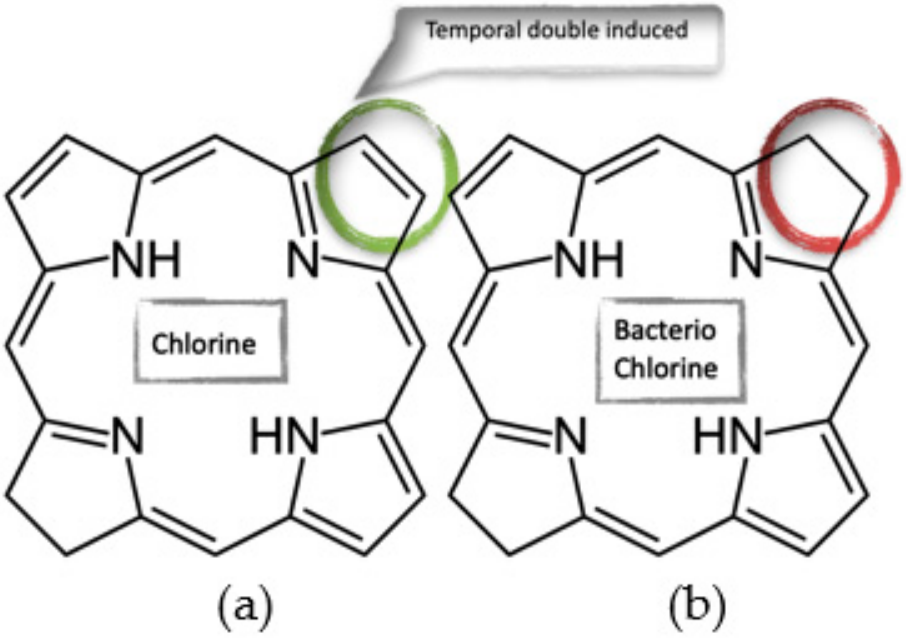

Figure 5. Chemical formula: (**a**)—chlorine; (**b**)—bacteriochlorine.

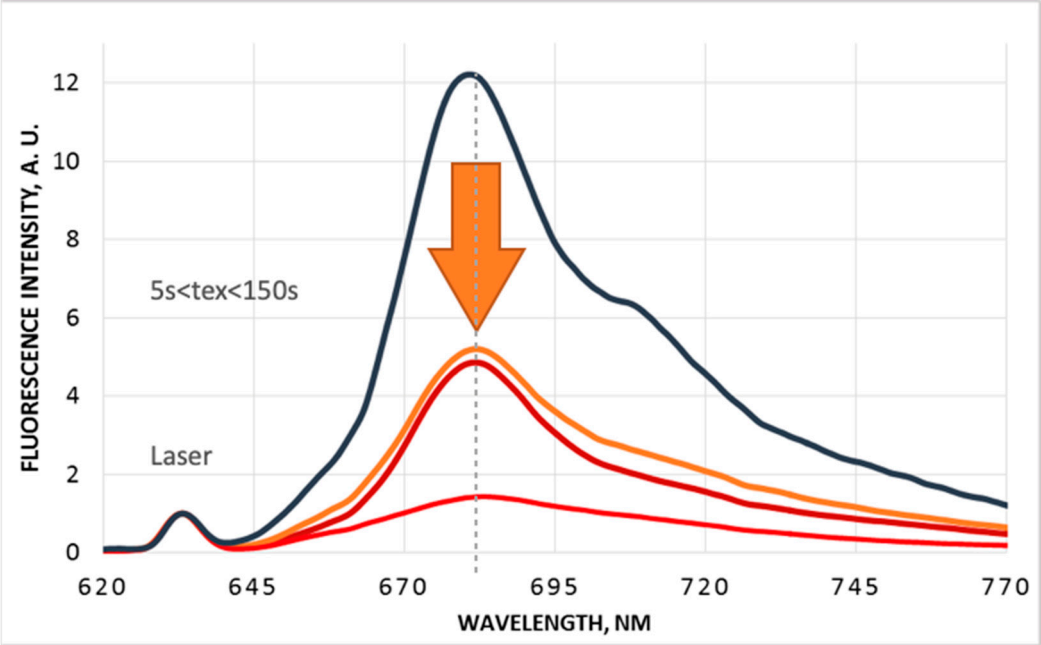

Figure 6. Time course of the luminescence spectrum of a hydroxyapatite-based implant coated with aluminum phthalocyanine nanoparticles (λex = 632.8 nm).

The time dynamics analysis of luminescence spectra for both types of crystalline nanoparticles revealed that initially photoinactive PS nanocrystals acquire luminescence ability when interacting with surface hydroxyapatite molecules, but the intensity of luminescence peak changes in time under the influence of excitation laser radiation. On the basis of these studies, it was concluded that the PS nanoparticles interact both among themselves and with the complex porous structure of the implant. Depending on the nature and force of interaction as well as localization and their own environment of nanoparticles they can take different positions in relation to each other and to the surface structure of hydroxyapatite, changing the spectroscopic properties. In this regard, we can draw a parallel between fluorescence processes and Raman and suggest that the spectral broadening of electronically excited states is related to a change in bond strength [23]. The structure of the molecules in this case does not undergo irreversible changes.

In the course of this work, the activation of bacteriochlorine and aluminum phthalocyanine nanoparticles was proved, which was evaluated by the signal level of photoluminescence in the control study mode. It was also found that there was a strong interaction between the surface molecules of the photosensitizer nanocrystals and the surface structure of hydroxyapatite, which will further rule out the possibility of leaching of the surface layer of the nanoparticles [24].

3.2. Studies of the Spectral Fluorescence Properties of Photosensitizers in Nanoform when Interacting with Cells

The intracellular distribution of bacteriochlorine nanoparticle colloid for glioma C6 and THP-1 cell cultures showed some differences.

3.2.1. THP-1 Immune System Cells

After the incubation of nanoparticle colloid with immune system cells (concentration of meso-tetra(3-pyridyl)bacteriochlorine solution in cell suspension 10 mg/L), no fluorescence signal corresponding to bacteriochlorine solution was registered after 2 h. However, under additional laser illumination with a wavelength of 510.6 nm, fluorescence with a maximum at 760 nm was observed. This effect can probably be explained by the transformation of crystalline nanoparticles of bacteriochlorine at the cell border due to the

absorption of laser radiation energy, due to which individual molecules of bacteriochlorine became capable of fluorescence (Figure 7).

The dynamics of accumulation and interaction of aqueous colloidal solution of bacteriochlorine nanoparticles with immune system cells were studied, in particular, the changes in fluorescence intensity of the studied drug during interaction with cells (concentration of bacteriochlorine nanoparticles solution in cell suspension 5 mg/L) were assessed.

Using confocal microscopy, the intracellular distribution of bacteriochlorine nanoparticles in human THP-1 monocytes cells of the immune system was investigated. The obtained microscopic image of intracellular distribution of colloidal nanoparticle solution demonstrates diffuse distribution of bacteriochlorine inside the cytoplasm of cells of the studied cellular structures (Figure 7).

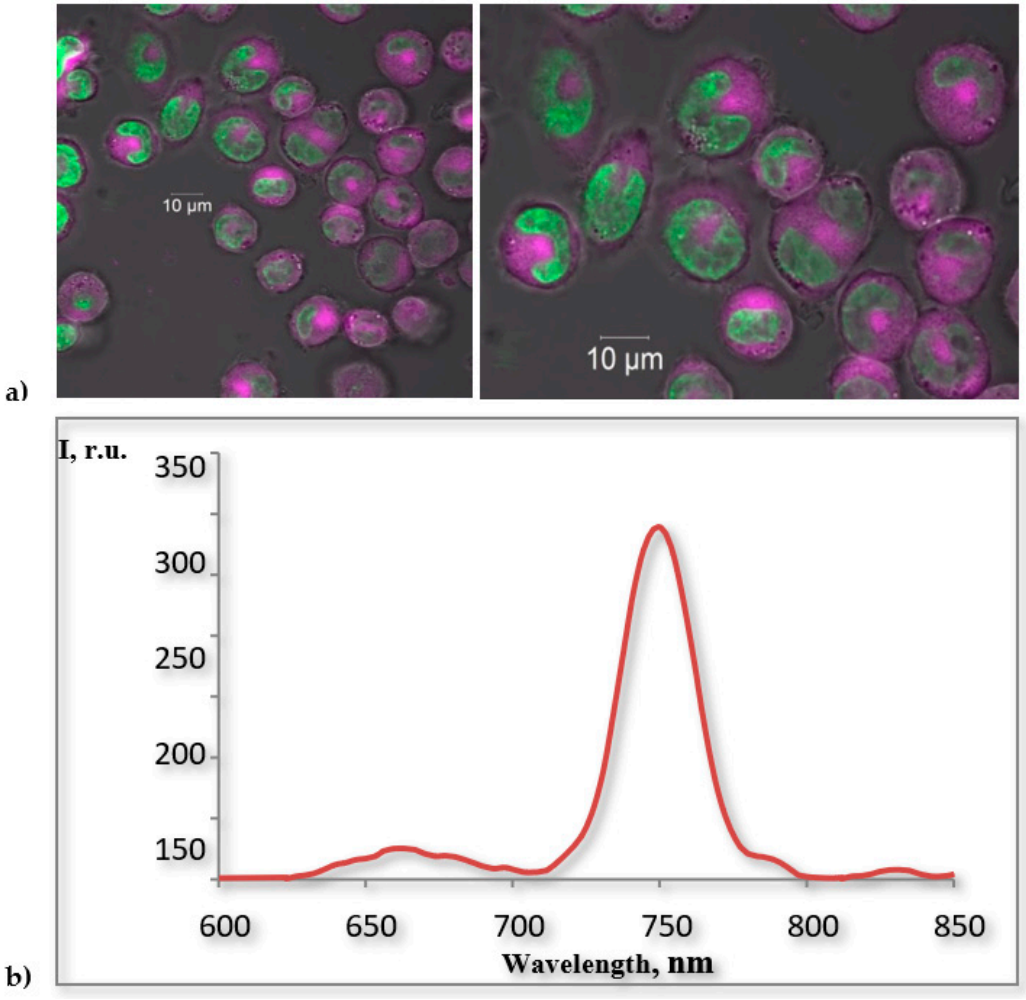

Figure 7. (**a**) Intracellular distribution of meso-tetra(3-pyridyl)bacteriochlorine nanoparticles in human THP-1 monocytes cells of the immune system. (**b**) Fluorescence spectrum of colloidal solution of meso-tetra(3-pyridyl)bacteriochlorine nanoparticles in macrophage cell medium when excited by laser irradiation (λ = 510.6 nm).

3.2.2. C6 Malignant Glioma Cells

Using confocal microscopy, the intracellular distribution of meso-tetra(3-pyridyl)bacteriochlorine nanoparticles in mouse glioma C6 brain tumor cells (concentration of meso-tetra(3-pyridyl)bacteriochlorine nanoparticles solution in cell suspension 5 mg/L) was investigated. The obtained microscopic image of the intracellular distribution of colloidal nanoparticle solution demonstrates diffuse distribution of bacteriochlorine inside the cytoplasm of cells of the studied cellular structures (Figure 8).

As previously mentioned, depending on the immediate environment, the surface molecules of the substance under study can have different spatial orientations or positions, which can be denoted as ortho- and parapositions. The interaction of nanoparticles with the membrane and cell organelles is due to the surface molecules, the configuration of which depends on the strength of this interaction with the cells. Thus, the surface molecules of nanoparticles may be retained on the surface or detached from the nanoparticle, leaving individual molecules in the form of bacteriochlorin or chlorinE6 in contact with cellular structures (Figure 9). Depending on the exact position taken by the surface molecules in contact with the cells, the preparation under study exhibits the spectroscopic properties of the bacteriochlorine or chlorineE6 molecule. The interaction between the surface molecules and biological objects, as well as with the implant surface is rather of physical nature due to the difference of Z potentials of the interacting surfaces. As a result, an induced electric dipole moment arises when they approach each other, which becomes compensated by changing the position of surface molecules.

The spectral range of 633–691 nm was used to estimate the fluorescence signal of chlorine molecules, and the spectral range of 691–758 nm was used to estimate the fluorescence signal of bacteriochlorine molecules (Figure 10).

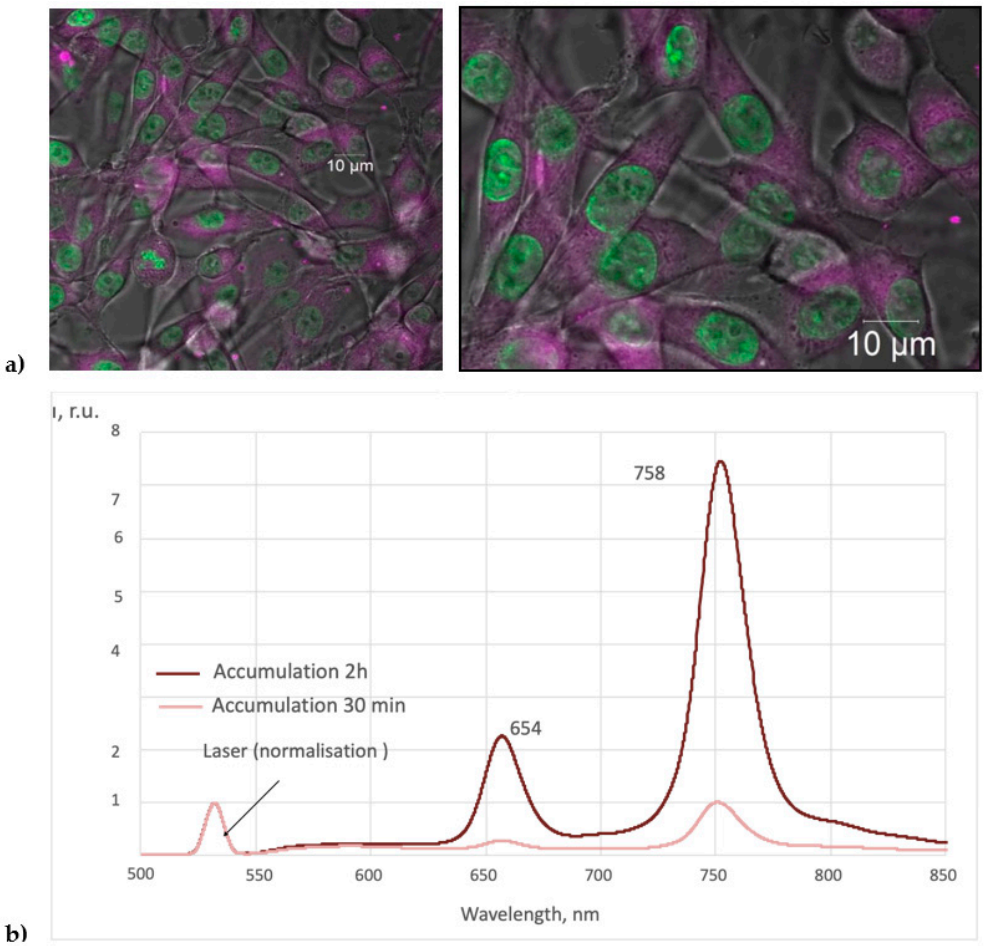

Figure 8. (**a**) Intracellular distribution of meso-tetra(3-pyridyl)bacteriochlorine nanoparticles in rat gliomaC6 cells. (**b**) Fluorescence spectrum of colloidal solution of meso-tetra(3-pyridyl)bacteriochlorine nanoparticles in rat gliomaC6 cells when excited by laser irradiation (λ = 510.6 nm).

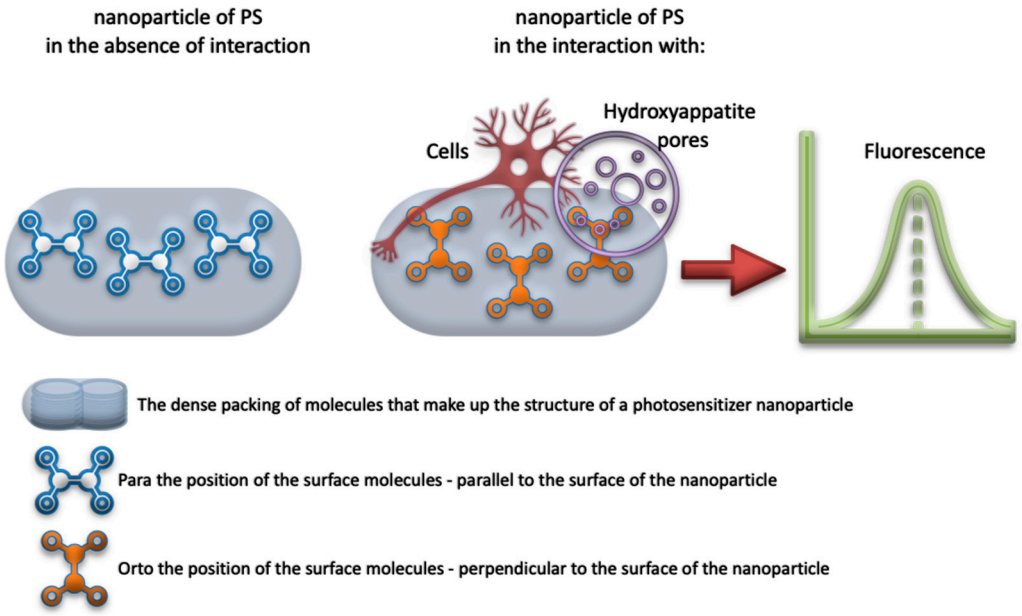

Figure 9. Schematic representation of a model of the transition process of surface molecules from para- to ortho-position with respect to the plane of a crystalline nanoparticle.

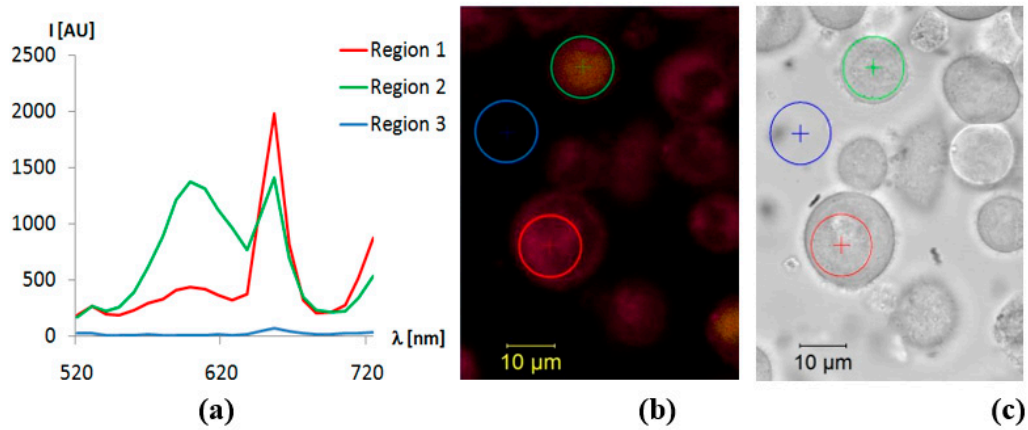

Figure 10. A fluorescence microscopic image (center) was obtained with spectral resolution under 514 nm laser excitation. Fluorescence spectra (left) correspond to selected areas: (**a**) cell accumulating meso-tetra(3-pyridyl)bacteriochlorine, (**b**) cell accumulating meso-tetra(3-pyridyl)bacteriochlorine with increased autofluorescence in the range of 600 nm, (**c**) background glow of culture medium. On the right is an image of the cells in transmitted light.

Experimental evaluation of changes in fluorescence intensity of bacteriochlorine nanoparticles (solution concentration of meso-tetra(3-pyridyl)bacteriochlorine nanoparticles in cell suspension 5 mg/L) in interaction with immune system cells (human THP-1 monocytes) and mouse brain tumor cancer cells (glioma C6) showed that the fluorescence intensity of molecules with chlorine spectroscopic properties is higher than the fluorescence intensity of bacteriochlorine molecules. The obtained time dependence allows us to conclude that the fluorescence intensity of nanoparticles varies in time in the media with different cell cultures in different ways (Figure 10). Thus, in experiments with mouse brain glioma cells, it was found that the fluorescence signal intensity of surface-active nanoparticle molecules, which assumed a position characterized by the spectroscopic properties of the chlorine molecule, changed little with time and within

After 24 h, a slight increase in signal intensity was recorded. The fluorescence intensity of bacteriochlorine molecules changes with time such that a period of fluorescence

kindling during the first 5 h of incubation and an elimination period after 5 h (5–24 h) of incubation with C6 glioma cells can be distinguished (Figure 11a). Experiments with immune system cells showed that both chlorine and bacteriochlorine molecules were characterized by a fluorescence kindling period during the first 5 h of incubation with cells and a burnout period when the preparation was incubated with cells for more than 5 h (5–24 h) (Figure 11b).

The interaction of molecular nanocrystals of bacteriochlorine with cells results in a fluorescence spectrum characteristic of bacteriochlorine solution. The aqueous colloid of bacteriochlorine nanocrystals, initially not phototoxic, under the conditions of cellular environment demonstrates the properties of a near-infrared photosensitizer. Using confocal microscopy, the diffuse distribution of bacteriochlorin within the cytoplasm of the cells. The studied bacteriochlorine is a promising compound for the preparation based on its molecular nanocrystals for use as a therapeutic agent with a great depth of photodynamic effect.

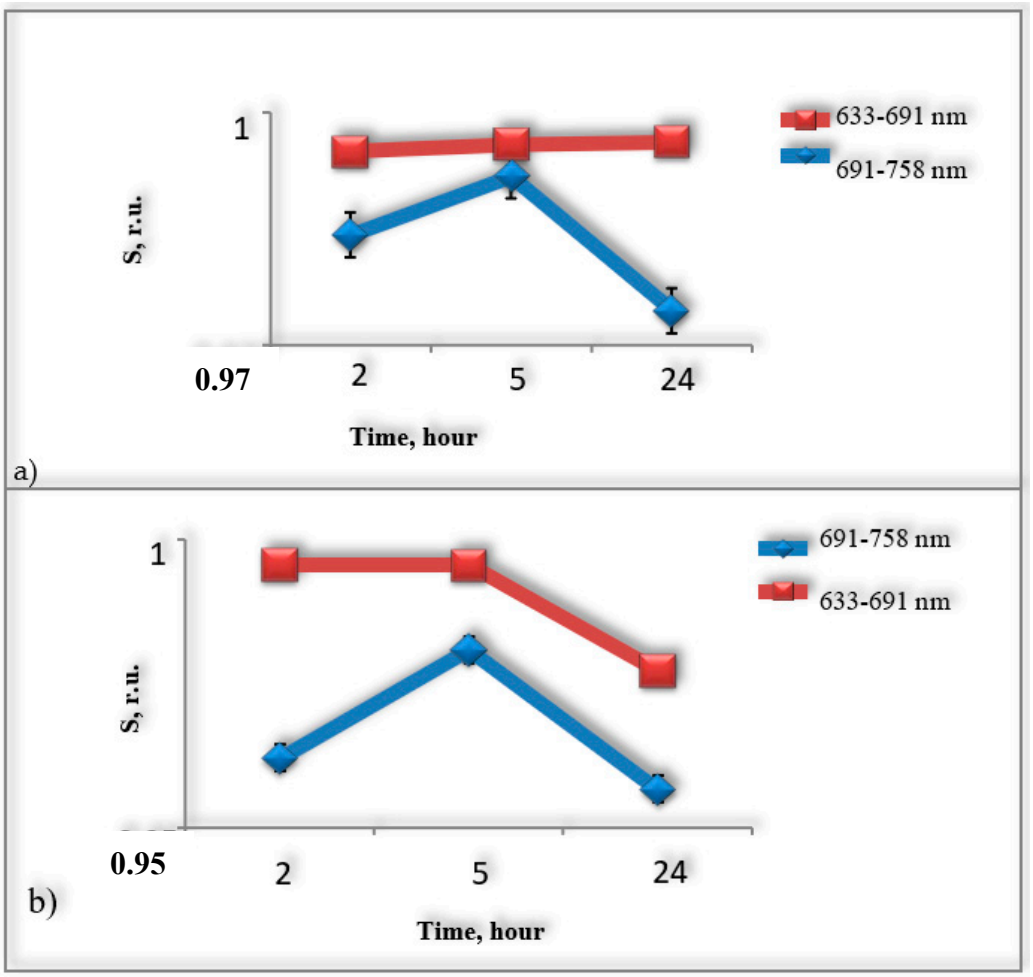

Figure 11. Time dependence of fluorescence signal intensity of surface active molecules of meso-tetra(3-pyridyl)bacteriochlorine nanoparticles: (**a**) in glioma C6 cells, (**b**) in human immune system cells THP-1 monocytes; 633–691 nm: fluorescent signal corresponding to surface active molecules, which have the spectroscopic features of a chlorine molecule; 691–758 nm: fluorescence signal corresponding to surface active molecules that have the spectroscopic features of a bacteriochlorin molecule the studied cellular structures was demonstrated. The studied bacteriochlorine was demonstrated to be a promising compound for the preparation based on its molecular nanocrystals to be used as a therapeutic agent with a great depth of photodynamic effect.

4. Discussion

The main purpose of the study was to find spectral and luminescent signs of binding of photosensitizer nanoparticles to the porous surface of the implant, as well as directly to biological objects. As seen, the first results show the promise of this tactic for the further development and clinical use of implants with a surface photo-sensitive coating to indicate the processes of inflammation and prevent their development.

These studies should provide a basis for the search of correspondence between the physical characteristics of photosensitizer fluorescence, namely, the dependence of the spectral composition and fluorescence intensity on the type of surface to which the photosensitizer binds, as well as on the type and number of cells, including immunocompetent nature as inflammation indicators. Fiber probes in this case play an important role in terms of local sensing of the implanted area. As a result, both a quantitative ratio of macrophages or the level of local inflammation will be established, but local photodestruction of inflammatory agents is also possible, which is also possible thanks to fiber probes and the targeted delivery of laser radiation.

It should be noted that, recently, there is a growing number of studies devoted to the role of immunity in the development of pathological complications in the implant area, up to the rejection of the implant [25–27]. Since systemic immune suppression is highly undesirable in the postoperative period, the question of local effects is very pressing in this area.

Especially in bone tissue, the role of macrophages in interfering with the engraftment process has been shown by researchers to be particularly frequent, i.e., they are a target [28–30].

In fact, immunity always interacts in one way or another with the implant as a foreign element to the biotissue [31]. Therefore, monitoring the course of the dialogue between the implant surface, namely the hydroxyapatite, and the immune cells is an important aspect both for practical purposes, such as the prevention of rejection, the restoration of the overall normal immune response, and for the fundamental purposes of investigating the root causes of inflammatory reactions of any localisation [32,33].

5. Conclusions

In the course of the study, it was shown that, based on the measurements of spectral characteristics and fluorescence intensity, it is possible to judge the nature of interaction of photosensitizer in nano-form with implant surface, as well as to monitor the inflammation processes, namely, the contribution of immune cells to the process of fluorescence generation. On the basis of this approach spectral characteristics of fluorescence of nano-photosensitizers in the near-infrared region of the spectrum, interacting both with pores of hydroxyappatite and with cancer and rumen cells, were obtained. In this context, the technique of analysis of the implant engraftment process and the level of inflammation by local fluorescence signal seems promising. Namely, the estimation of intensity and spectral composition of fluorescence allowed us to estimate the character of the interaction of the surface molecules of the nanoforms of photosensitizers with the nearest microenvironment, that in its turn will be a kind of marker for the analysis of the nature of microenvironment (cancer immune cell). In turn, the fiber part of the implant, as well as the diagnostic fiber probe, allowed us to assess local inflammation with great accuracy, which in turn opens up the possibility of local immunosuppression using phototherapy.

Author Contributions: Conceptualization, Y.M.; methodology, V.L.; software, I.R.; validation, Y.M. and I.R.; formal analysis, D.F. and S.K.; investigation, Y.M. and I.R. and A.S.; resources, L.B. and V.L.; data curation, V.L.; writing—original draft preparation, Y.M.; writing—review and editing, Y.M.; visualization, I.R.; supervision, L.B. and V.L.; project administration, L.B. and Y.M.; funding acquisition, L.B. and Y.M. All authors have read and agreed to the published version of the manuscript.

Funding: This research was funded by RFBR according to the research project No. 21-52-15025 and partly by IEA (International Emerging Action) CNRS grant 00534.

Institutional Review Board Statement: Animal care protocols were used in accordance with the guidelines of the European Convention for the Protection of Vertebrate Animals used for Experimental and Other Scientific Purposes (Strasbourg, 18.III.1986).

Informed Consent Statement: Not applicable.

Data Availability Statement: Maklygina, Y.S. Development of Spectral Fluorescent Methods of Diagnostics and Therapy of Deep Brain Tumors. Ph.D. Thesis, Prokhorov General Physics Institute of the Russian Academy of Sciences, 119991, Moscow, Russia, 2019.

Conflicts of Interest: The authors declare no conflict of interest.

References

1. Chen, K. *Luorescent Analytical Method, Xiamen University*; Science Publishing House: New York, NY, USA, 1990.
2. Korbelik, M.; Krosl, G. Br Photofrin accumulation in malignant and host cell populations of various tumours. *J. Cancer* **1996**, *73*, 506–513. [CrossRef] [PubMed]
3. Gao, S.; Lu, R.; Wang, X.; Chou, J.; Wang, N.; Huai, X.; Wang, C.; Zhao, Y.; Chen, S. Immune response of macrophages on super-hydrophilic TiO2 nanotube arrays. *J. Biomater. Appl.* **2020**, *34*, 1239–1253. [CrossRef]
4. Sharma, S.; Jajoo, A.; Dube, A. 5-Aminolevulinic acid-induced protoporphyrin-IX accumulation and associated phototoxicity in macrophages and oral cancer cell lines. *J. Photochem. Photobiol. B Biol.* **2007**, *88*, 156–162. [CrossRef]
5. Demidova, T.N.; Hamblin, M.R. Macrophage-Targeted Photodynamic Therapy. *Int. J. Immunopathol. Pharmacol.* **2004**, *17*, 117–126. [CrossRef]
6. Schastak, S.; Jean, B.; Handzel, R.; Kostenich, G.; Hermann, R.; Sack, U.; Orenstein, A.; Wang, Y.-S.; Wiedemann, P. Improved pharmacokinetics, biodistribution and necrosis in vivo using a new near infra-red photosensitizer: Tetrahydroporphyrin tetratosylat. *J. Photochem. Photobiol. B Biol.* **2005**, *78*, 203–213. [CrossRef] [PubMed]
7. Schastak, S.; Yafai, Y.; Geyer, W.; Kostenich, G.; Orenstein, A.; Wiedemann, P. Initiation of apoptosis by photodynamic therapy using a novel positively charged and water soluble near infra-red photosensitizer and white light irradiation. *Methods Find. Exp. Clin. Pharmacol.* **2008**, *30*, 17–23. [CrossRef] [PubMed]
8. Maawy, A.A.; Hiroshima, Y.; Zhang, Y.; Heim, R.; Makings, L.; Garcia-Guzman, M.; Luiken, G.A.; Kobayashi, H.; Hoffman, R.M.; Bouvet, M. Near Infra-Red Photoimmunotherapy with Anti-CEA-IR700 Results in Extensive Tumor Lysis and a Significant Decrease in Tumor Burden in Orthotopic Mouse Models of Pancreatic Cancer. *PLoS ONE* **2015**, *10*, e0121989. [CrossRef] [PubMed]
9. Maklygina, Y.; Romanishkin, I.; Skobeltsin, A.; Farrakhova, D.; Loschenov, V. Phototherapy of Brain Tumours Using a Fibre Optic Neurosystem. *Photonics* **2021**, *8*, 462. [CrossRef]
10. Yoon, I.; Li, J.; Shim, Y.K. Advance in Photosensitizers and Light Delivery for Photodynamic Therapy. *Clin. Endosc.* **2013**, *46*, 7–23. [CrossRef]
11. Abrahamse, H.; Hamblin, M.R. New photosensitizers for photodynamic therapy. *Biochem. J.* **2016**, *473*, 347–364. [CrossRef]
12. Assi, H.; Candolfi, M.; Lowenstein, P.R.; Castro, M.G. Rodent Glioma Models: Intracranial Stereotactic Allografts and Xenografts. *Neuromethods* **2012**, *77*, 229–243. [CrossRef] [PubMed]
13. McKay, C.M. Brain Plasticity and Rehabilitation with a Cochlear Implant. *Cochlear Implant. Hear. Preserv.* **2018**, *81*, 57–65. [CrossRef]
14. Spennato, P.; Canella, V.; Aliberti, F.; Russo, C.; Ruggiero, C.; Nataloni, A.; Lombardo, M.; Cinalli, G. Hydroxyapatite ceramic implants for cranioplasty in children: A retrospective evaluation of clinical outcome and osteointegration. *Child's Nerv. Syst.* **2020**, *36*, 551–558. [CrossRef]
15. Beuriat, P.-A.; Lohkamp, L.-N.; Szathmari, A.; Rousselle, C.; Sabatier, I.; Di Rocco, F.; Mottolese, C. Repair of Cranial Bone Defects in Children Using Synthetic Hydroxyapatite Cranioplasty (CustomBone). *World Neurosurg.* **2019**, *129*, e104–e113. [CrossRef]
16. Stefini, R.; Zanotti, B.; Nataloni, A.; Martinetti, R.; Scafuto, M.; Colasurdo, M.; Tampieri, A. The Efficacy of Custom-Made Porous Hydroxyapatite Prostheses for Cranioplasty: Evaluation of Postmarketing Data on 2697 Patients. *J. Appl. Biomater. Funct. Mater.* **2015**, *13*, 136–144. [CrossRef] [PubMed]
17. Zanotti, B.; Zingaretti, N.; Verlicchi, A.; Robiony, M.; Alfieri, A.; Parodi, P.C. Cranioplasty. *J. Craniofacial Surg.* **2016**, *27*, 2061–2072. [CrossRef]
18. Schmitt, D.; Blanck, O.; Gauer, T.; Fix, M.K.; Brunner, T.B.; Fleckenstein, J.; Loutfi-Krauss, B.; Manser, P.; Werner, R.; Wilhelm, M.L.; et al. Technological quality requirements for stereotactic radiotherapy: Expert review group consensus from the DGMP Working Group for Physics and Technology in Stereotactic Radiotherapy. *Strahlenther Onkol.* **2020**, *196*, 421–443. [CrossRef]
19. Farrakhova, D.S.; Kuznetsova, J.O.; Loschenov, V.B. The study of laser induced fluorescence of tooth hard tissues with aluminum phthalocyanine nanoparticles. *J. Physics Conf. Ser.* **2016**, *737*, 12048. [CrossRef]
20. Bystrov, F.G.; Makarov, V.I.; Pominova, D.; Ryabova, A.V.; Loschenov, V.B. Analysis of photoluminescence decay kinetics of aluminum phthalocyanine nanoparticles interacting with immune cells. *Biomed. Photon.* **2016**, *5*, 3–8. [CrossRef]
21. Lakowicz, J.R. (Ed.) *Principles of Fluorescence Spectroscopy*; Springer: Boston, MA, USA, 2013. [CrossRef]
22. Zhenwang, L.; ZhenLu, C.; Jianyan, L. The PT Dye Molecular Structure and Its Chromophoric Luminescence Mechanism. Available online: https://www.ndt.net/article/wcndt00/papers/idn105/idn105.htm (accessed on 1 November 2021).

23. Ramachandran, K.; Kumari, A.; Acharyya, J.N.; Chaudhary, A. Study of photo induced charge transfer mechanism of PEDOT with nitro groups of RDX, HMX and TNT explosives using anti-stokes and stokes Raman lines ratios. *Spectrochim. Acta Part A Mol. Biomol. Spectrosc.* **2021**, *251*, 119360. [CrossRef]
24. Maklygina, Y.S. Development of Spectral Fluorescent Methods of Diagnostics and Therapy of Deep Brain Tumors. Ph.D. Thesis, Prokhorov General Physics Institute of the Russian Academy of Sciences, Moscow, Russia, 10 July 2019.
25. Mahon, O.R.; Browe, D.; Gonzalez-Fernandez, T.; Pitacco, P.; Whelan, I.T.; Von Euw, S.; Hobbs, C.; Nicolosi, V.; Cunningham, K.T.; Mills, K.; et al. Nano-particle mediated M2 macrophage polarization enhances bone formation and MSC osteogenesis in an IL-10 dependent manner. *Biomaterials* **2020**, *239*, 119833. [CrossRef]
26. Jamalpoor, Z.; Asgari, A.; Lashkari, M.H.; Mirshafiey, A.; Mohsenzadegan, M. Modulation of Macrophage Polarization for Bone Tissue Engineering Applications. *Iran. J. Allergy Asthma Immunol.* **2018**, *17*, 398–408. [CrossRef]
27. Fernandes, T.L.; Gomoll, A.H.; Lattermann, C.; Hernandez, A.J.; Bueno, D.F.; Amano, M.T. Macrophage: A Potential Target on Cartilage Regeneration. *Front. Immunol.* **2020**, *11*, 111. [CrossRef]
28. Szcześ, A.; Holysz, L.; Chibowski, E. Synthesis of hydroxyapatite for biomedical applications. *Adv. Colloid Interface Sci.* **2017**, *249*, 321–330. [CrossRef] [PubMed]
29. Zhao, Z.; Zhao, Q.; Gu, B.; Yin, C.; Shen, K.; Tang, H.; Xia, H.; Zhang, X.; Zhao, Y.; Yang, X.; et al. Minimally invasive implantation and decreased inflammation reduce osteoinduction of biomaterial. *Theranostics* **2020**, *10*, 3533–3545. [CrossRef]
30. Zhang, Y.; Cheng, X.; Jansen, J.A.; Yang, F.; Beucken, J.J.V.D. Titanium surfaces characteristics modulate macrophage polarization. *Mater. Sci. Eng. C* **2019**, *95*, 143–151. [CrossRef] [PubMed]
31. O'Brien, F.J. Biomaterials & scaffolds for tissue engineering. *Mater. Today* **2011**, *14*, 88–95. [CrossRef]
32. Lebre, F.; Sridharan, R.; Sawkins, M.J.; Kelly, D.J.; O'Brien, F.J.; Lavelle, E.C. The shape and size of hydroxyapatite particles dictate inflammatory responses following implantation. *Sci. Rep.* **2017**, *7*, 2922. [CrossRef]
33. Ong, S.-M.; Biswas, S.K.; Wong, S.-C. MicroRNA-mediated immune modulation as a therapeutic strategy in host-implant integration. *Adv. Drug Deliv. Rev.* **2015**, *88*, 92–107. [CrossRef]